

## Brief Reports

*Brief Reports are accounts of completed research which, while meeting the usual Physical Review standards of scientific quality, do not warrant regular articles. A Brief Report may be no longer than four printed pages and must be accompanied by an abstract. The same publication schedule as for regular articles is followed, and page proofs are sent to authors.*

### Real-time probe of reaction centers in solid combustions on the subsecond time scale

R. Frahm

*Hamburger Synchrotronstrahlungslabor HASYLAB at DESY, Notkestrasse 85, D-2000 Hamburg 52, Germany*

Joe Wong

*Hamburger Synchrotronstrahlungslabor HASYLAB at DESY, Notkestrasse 85, D-2000 Hamburg 52, Germany  
and Lawrence Livermore National Laboratory, University of California, P.O. Box 808, Livermore, California 94551*

J. B. Holt, E. M. Larson, B. Rupp, and P. A. Waide

*Lawrence Livermore National Laboratory, University of California, P.O. Box 808, Livermore, California 94551*

(Received 30 January 1992)

A quick-scanning extended x-ray-absorption fine-structure (QEXAFS) technique has been devised to follow the local atomic coordination changes about selected reactants in a class of highly exothermic solid-combustion reactions. Real-time EXAFS measurements during the combustion were made in the time frame of a few seconds. By tuning the monochromator to a specific energy, at which maximum changes occur in an EXAFS feature of an element transforming from the reactant to the product phase, a time resolution of 20 ms was achieved. The  $\text{Ni} + \text{Al} \rightarrow \text{NiAl}$  reaction has been investigated in some detail in light of a possible intermediate phase in the so-called "after-burn" region. The present QEXAFS findings together with the recent time-resolved diffraction data on the same system lends experimental insights into the structural macrokinetics of this class of combustion systems.

Solid-combustion synthesis (SCS) is a class of fascinating high-temperature reactions in which at least one of the reactants is a solid. The underlying basis is the ability of highly exothermic reactions to sustain themselves in the form of a reaction or combustion front. The temperature of the combustion front can be extremely high ( $\sim 4000$  K) and the rate of propagation can be relatively rapid ( $\sim 100$  mm/s). Such SCS processes permit an opportunity to study phase transformations and solid-state reaction dynamics at extreme thermal gradients ( $10^5$  K/cm) and under conditions such that adiabatic conditions are conveniently invoked in theoretical analysis. This field of study was pioneered by Merzhanov, Borovinskaya, and co-workers in the Soviet Union about two decades ago<sup>1</sup> and has also been called self-propagating high-temperature synthesis (SHS) by the Russian school. A number of reviews on SHS have recently been published.<sup>2-4</sup>

Because of the high rate of combustion and extreme thermal conditions, the chemical kinetics and dynamics of phase transformations at the combustion front are not well understood.<sup>3,4</sup> This is true even of the simple binary  $A + B \rightarrow AB$  type of solid-combustion reactions. We have recently developed a time-resolved x-ray-diffraction (TR-XRD) technique using synchrotron radiation to investigate the phase transformation of some simple binary reactions.<sup>5,6</sup> These TR-XRD results are very encouraging and enable for the first time a "look" at SCS reactions

in the course of transformation from reactant to product (via intermediate, if it exists) *in situ* and in real time down to a 10-ms time frame.

In this paper, we report results obtained with a time-resolved x-ray spectroscopic probe, the quick-scanning extended x-ray-absorption fine-structure (QEXAFS) method,<sup>7,8</sup> to monitor the local atomic coordination changes about the Ni reactant in the  $\text{Ni} + \text{Al} \rightarrow \text{NiAl}$  combustion reaction. The experiments were performed at Stanford Synchrotron Radiation Laboratory (SSRL) at the wiggler beamline 10-2.<sup>9</sup> The electron storage ring SPEAR was operated at 3.0 GeV with injection currents of about 100 mA. The 31-pole wiggler was operated at a magnetic field of 1.49T. The synchrotron beam was monochromatized by two Si(111) crystals mounted on a single goniometer. The crystals could be detuned with respect to each other using a piezo crystal to reduce the amount of harmonics in the Bragg reflected beam.<sup>10</sup> The spectrometer resolution was  $\sim 1$  eV at the Ni K edge at 8333 eV. The flux of the monochromatic beam was of the order of  $10^{11}$  photons/s. Before entering the sample chamber, the monochromatized beam first passed through two short ion chambers, one for monitoring the intensity of the incident beam and the second for energy calibration with a metal foil, if needed. The absorption of the sample was recorded in the fluorescence mode using the detector developed by Lytle.<sup>11</sup> All signals were amplified by current amplifiers and converted into a fre-

quency, which was counted for preset periods of time.

In a conventional EXAFS experiment, the monochromator is moved in small energy steps from lower to higher energies to yield a point-by-point spectrum. Such a measurement scanning over 1000 eV typically takes about 10–15 min. A parallel measurement of a whole absorption spectrum within several ms is, in principle, possible using the energy dispersive EXAFS method with a bent crystal monochromator and position-sensitive detector setup.<sup>12,13</sup> This technique, however, is limited to the transmission geometry and to very homogeneous samples and cannot be applied in the current case due to the large sample dimensions (cm) required to sustain self-propagation of the combustion. The QEXAFS technique allows EXAFS measurements to be made not only in the transmission mode, but also in the fluorescence as well as in the total electron yield modes in a matter of a few seconds. The QEXAFS setup is also relatively simple, requiring a conventional, but stable, monochromator and normal EXAFS setup outlined above. To achieve the quick-scanning mode, the monochromator is slewed continuously at high speed by means of a microstepping mechanism.<sup>7</sup> Each absorption value is integrated for typically 0.01–0.05 s, and the corresponding (average) photon energy can easily be determined from the Bragg angle of the monochromator. Even with such short collection times, the quality of the data is comparable to conventional point-by-point scans. This is because, in general, the noise in EXAFS measurements is not governed by photon statistics, but by experimental factors, such as mechanical instabilities.<sup>14</sup> Thus, even surface studies are feasible with time resolutions in the second range.<sup>15,16</sup> An additional advantage of the QEXAFS approach is that other experimental parameters such as temperatures, magnetic fields, etc., can be recorded easily and synchronously with the absorption spectrum.

A schematic of the sample configuration is shown in

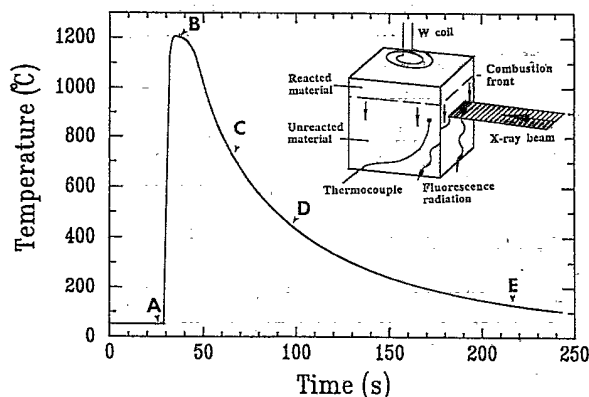


FIG. 1. Temperature-time profile for the  $\text{Ni} + \text{Al} \rightarrow \text{NiAl}$  reaction measured synchronously with a W/W+26% Re microthermocouple. Points A, B, C, D, and E represent the temperatures and times at which various selected QEXAFS scans are extracted in the path of the reaction shown in Figs. 2 and 3.  $t=0$  corresponds to the start of the QEXAFS measurements. The inset is a schematic of sample configuration used in present QEXAFS measurements of SCS reactions.

the inset of Fig. 1. The samples, in the form of a 19-mm cube, were pressed from dry-mixed 50-50 atomic mixtures of Ni and Al powders having a pressed density of  $\sim 55\%$  of the theoretical value. The average particle sizes for Ni and Al were 5 and 20  $\mu\text{m}$ , respectively. The QEXAFS data collection was first initiated at ambient temperatures, and within 20–30 s the sample was ignited electrically from the top by a W coil. A W/W+26% Re microthermocouple was used to record the temperature-time profile synchronously with the QEXAFS data collection.

In the QEXAFS mode, the fluorescence spectra were recorded from  $-40$  to  $+160$  eV with respect to the Ni K edge at 8333 eV. Each spectrum took  $\sim 3$  s to record and some  $\sim 3$ -s delay was used to store and display the data on the computer giving a total of 6s between consecutive scans. For the Ni+Al reaction it was found consistently that the fcc Ni reactant is transformed (reacted) to a Ni-Al phase within one QEXAFS frame of 6 s. The temperature profile vs time is shown in Fig. 1. At  $t=0$ , the QEXAFS data collection was triggered. The sharp rise from A to B in the profile marks the arrival of the combustion front at the region of the sample illuminated by the synchrotron beam.

In Fig. 2, the extracted EXAFS signals corresponding to points A, B, C, D, and E along the temperature-time profile of Fig. 1 are plotted. Curve A corresponds to that of the Ni reactant at ambient temperature which is fcc in structure. At the next QEXAFS frame (curve B), the sample has attained its maximum temperature of 1190°C, marking passage of the combustion front in the region of the sample illuminated by the synchrotron beam. Within this time frame, fcc Ni is transformed (reacted) to a different structure, being dissolved in liquid aluminum which melts at 660°C. Evidence for the Ni dissolution in the molten Al is discussed in more detail below in the constant energy experiments. Curves C, D, and E correspond to specimen temperatures at 730, 410, and 110°C, respectively, and show a progressive increase in the EXAFS signal at higher- $k$  values denoting noticeable changes in the local coordination of the Ni in the NiAl product as it cools.

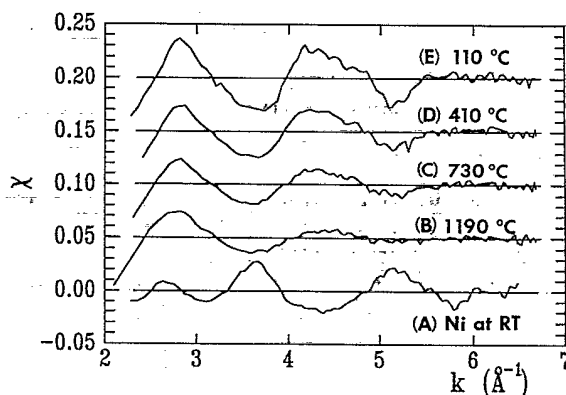


FIG. 2. Extracted Ni K-edge EXAFS signals along the temperature profile shown in Fig. 1. (A) Ni reactant at ambient temperature; (B) Ni-Al phase at 1190°C; (C)–(E) NiAl cooling down to various temperatures.

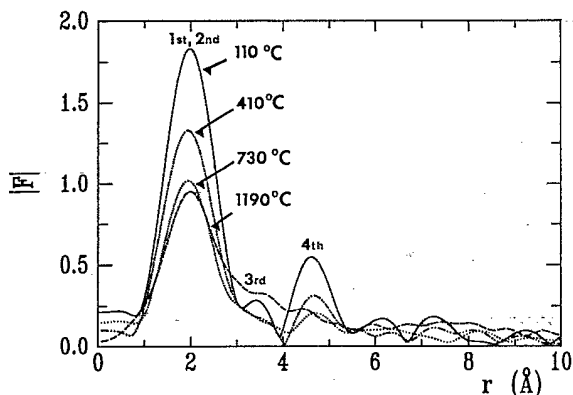


FIG. 3. Fourier transforms of Ni K-edge EXAFS signals shown in Fig. 2, curves (B)–(E) of a Ni–Al phase at high temperature and from NiAl formed in the after-burn region, respectively.

Fourier transforms of the EXAFS curves B, C, D, and E shown in Fig. 2 are plotted in Fig. 3. From the shell-by-shell coordination geometry of Ni in the NiAl structure (Table I), as calculated with a recently developed microcomputer program SEXIE,<sup>17</sup> the first peak at  $\sim 2$  Å corresponds to the first and second coordination shells about the Ni center in NiAl which has the CsCl structure.<sup>18</sup> The Fourier peaks at  $\sim 3.5$  Å and  $\sim 4.5$  Å are those of the third and fourth shells. The first radial structural feature is the only dominant feature at the maximum reaction temperature at 1190°C and increases in magnitude as the reacted specimen cools showing a reduction in the Debye-Waller factor in the measured EXAFS signal. At 730°C and some 30 s after the passage of the combustion front, the fourth shell becomes apparent and increases in magnitude with further temperature decrease. This instance marks the low-temperature limit for the formation of longer-range order about the Ni center as the NiAl product is being formed. At 410°C, the third shell appears as a shoulder and becomes resolved at 110°C. This series of QEXAFS measurements reveals the time events of coordination changes about the Ni center in the so-called “after-burn” region well after the combustion front has swept through the specimen. To confirm the Debye-Waller effect on the observed EXAFS as the system cooled from its maximum reaction temperature, the NiAl product was reheated from room temperature to 750°C. An identical EXAFS spectrum and Fourier transform were obtained as the one shown in Figs. 2 (C) and 3, respectively. It must be noted

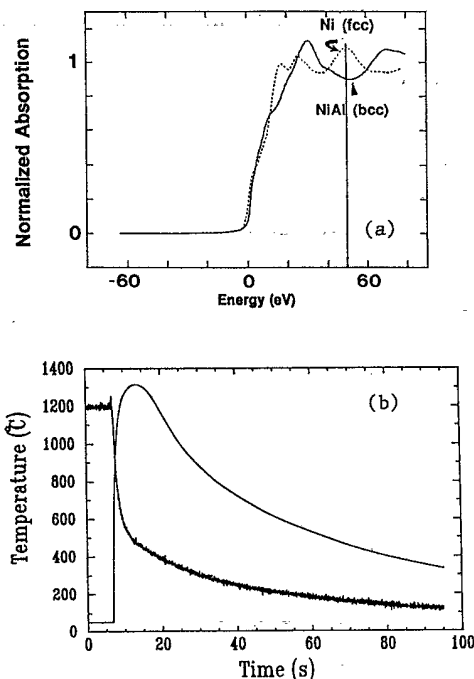


FIG. 4. (a) Normalized Ni K-edge near-edge absorption spectra for fcc Ni metal and bcc NiAl. (b) Ni K fluorescence decay measured with constant photon energy at 8381 eV vs time in the course of the Ni+Al combustion. The smooth line is the corresponding temperature profile measured synchronously.

that, with the fluorescence detection scheme, the measured EXAFS amplitudes of bulk (concentrated) samples are reduced due to self-absorption.<sup>19,20</sup> This effect, however, does not invalidate our temperature-dependent results since we are looking at a systematic trend in this combustion system.

The velocity of combustion front for the Ni+Al reaction was measured by a video camera to be  $> 20$  mm/s. Therefore, within 1 s the combustion front has swept through the whole length of the 19-mm-long sample. In order to better time resolve the dynamical event at the combustion zone, we employed a constant energy scan mode by tuning the monochromator to an energy which exhibits a sizable variation of an EXAFS feature from reactant to product. As plotted in Fig. 4(a), the normalized Ni x-ray absorption near-edge structure (XANES) transmission spectra for fcc Ni metal and for bcc NiAl show a change of the EXAFS amplitude from a max-

TABLE I. Ni coordination shells in NiAl ( $Pm\bar{3}m$ ,  $a = 2.8864$  Å) to 6.5 Å.

Shell	Neighbor	Coord. no.	Distance (Å)	Coord. geometry
1	Al	8	2.4997	Cubic
2	Ni	6	2.8864	Octahedral
3	Ni	12	4.0820	Simple cuboctahedron
4	Al	24	4.7866	Hexa-cuboctahedron
5	Ni	8	4.9994	Cubic
6	Ni	6	5.7728	Octahedral
7	Al	24	6.2908	Hexa-cuboctahedron
8	Ni	24	6.4542	Hexa-cuboctahedron

imum in Ni metal to a minimum in the NiAl compound at 48 eV above the Ni K edge. The variation of the x-ray fluorescence signal was then measured at a 20-ms time frame in the course of the combustion. The intensity data together with the temperature profile measured concurrently are plotted in Fig. 4(b). Again,  $t=0$  corresponds to triggering of the x-ray measurement. The intensity vs time curve consists of a sharp decay in the period  $t=7-12$  s, during which time the system attained its maximum temperature upon passage of the combustion front, showing clearly that the Ni reactant was transformed before the maximum temperature was reached. This was then followed by a slow intensity decay as the temperature of the system fell from its maximum value to end of the measurement at 95 s.

The QEXAFS results may now be correlated with earlier TR-XRD data for this system.<sup>5</sup> In the TR-XRD experiments, the strongest Ni(111) Bragg peak disappears within 3 s after passage of the combustion front, during which time the temperature of the system rises to the maximum temperature. The melting point of Al is 660°C. Thus, the initiate sharp intensity decay shown in Fig. 4(b) may be understood in terms of a phase transformation from fcc Ni metal to some Al-Ni phase due to its solution in the molten Al in the time interval taken by the system to attain its maximum temperature. Furthermore, from the TR-XRD data, the bcc NiAl final product is observed (formed) 10 s after passage of the combustion front, which, in accordance with the temperature profile shown in Fig. 4(b) occurs a few seconds after the system has attained its maximum temperature. This is also borne out in the Fourier transform of the QEXAFS data at 730°C and lower temperatures shown in Fig. 3.

The slow intensity decay beyond 20 s shown in Fig. 4(b) may therefore be attributed to a reduction in the Debye-Waller factor of the Ni EXAFS in NiAl with temperature decrease, which, in turn, increases the downward movement of the minimum feature in the NiAl EXAFS at 8381 eV shown in Fig. 4(a). The whole intensity-decay feature at constant energy is reproducible at both 8381 and 8347 eV.

In summary, we have employed an x-ray-absorption measurement in an attempt to time resolve the dynamics of local atomic coordination about a given reacting constituent element in solid combustion reactions. For the Ni+Al reaction, an energy scan QEXAFS in the time frame of a few seconds are useful to elucidate changes in the first few coordination spheres in the after-burn region. Using a constant energy detection mode, we achieved a time resolution of 20 ms to gain some insight into the dynamics events at the combustion front. Together with TR-XRD measurements, we are now beginning to explore and gain experimental insight into the structural macrokinetics of the combustion front in this class of fascinating solid combustions. With high fluxes of the third-generation synchrotron sources, faster computers, and faster detectors,<sup>21</sup> it is possible to investigate phase transformations and chemical dynamics in condensed matter with time resolution in the  $\mu$ s regime using this x-ray-absorption technique.

This work was supported by the U.S. Department of Energy (DOE) under Contract No. W-7405-ENG-48. R.F. is grateful to LLNL for hospitality and support during an extended stay. J.W. is grateful to the Alexander von Humboldt Stiftung for financial support.

<sup>1</sup>A. G. Merzhanov and I. P. Borovinskaya, Dokl. Akad. Nauk SSSR 204, 366 (1972).

<sup>2</sup>Z. A. Munir, Ceram. Bull. 27, 342 (1988).

<sup>3</sup>Z. A. Munir and U. Anselmi-Tamburini, Mater. Sci. Rep. 3, 277 (1989).

<sup>4</sup>A. G. Merzhanov, in *Combustion and Plasma Synthesis of High-Temperature Materials*, edited by Z. A. Munir and J. B. Holt (VCH, New York, 1990), pp. 1-53.

<sup>5</sup>Joe Wong, E. M. Larson, J. B. Holt, P. A. Waide, B. Rupp, and R. Frahm, Science 249, 1406 (1990).

<sup>6</sup>E. M. Larson, P. A. Waide, and Joe Wong, Rev. Sci. Instrum. 62, 53 (1991).

<sup>7</sup>R. Frahm, Nucl. Instrum. Methods A 270, 578 (1988).

<sup>8</sup>R. Frahm, Rev. Sci. Instrum. 60, 2515 (1989).

<sup>9</sup>V. Karpenko, J. H. Kinney, S. Kulkarni, K. Neufeld, C. Poppe, K. G. Tirsell, J. Wong, J. Cerino, T. Troxel, J. Yang, E. Hoyer, M. Green, D. Humphries, S. Marks, and D. Plate, Rev. Sci. Instrum. 60, 1451 (1989).

<sup>10</sup>G. Materlik and V. O. Kostroun, Rev. Sci. Instrum. 51, 86 (1980).

<sup>11</sup>F. W. Lytle, R. B. Greegor, D. Sandstrom, E. Marques, J. Wong, C. Spiro, G. Huffman, and F. Huggins, Nucl. Instrum. Methods 226, 542 (1984).

<sup>12</sup>R. P. Phizackerley, Z. U. Rek, G. B. Stephenson, S. D. Conradson, K. O. Hodgson, T. Matsushita, and M. Oyanagi, J. Appl. Cryst. 16, 220 (1983).

<sup>13</sup>E. Dartyge, C. Depaule, J. M. Dubuisson, A. Fontaine, A. Jucha, P. Leboucher, and G. Tourillon, Nucl. Instrum. Methods A 246, 452 (1986).

<sup>14</sup>F. W. Lytle and R. B. Greegor, in *X-ray Absorption Fine Structure*, edited by S. S. Hasnain (Horwood, New York, 1991), p. 625.

<sup>15</sup>R. Frahm, in *X-ray Absorption Fine Structure*, edited by S. S. Hasnain (Horwood, New York, 1991), p. 731.

<sup>16</sup>R. Frahm, T. W. Barbee, and W. Warburton, Phys. Rev. B 44, 2822 (1991).

<sup>17</sup>B. Rupp, B. Smith, and Joe Wong, J. Appl. Cryst. 24, 263 (1991).

<sup>18</sup>P. Villars and L. D. Calvert, *Pearson's Handbook of Crystallographic Data for Intermetallic Phases* (American Society for Metals, Metals Park, OH, 1985), p. 1038.

<sup>19</sup>J. Goulon, C. Goulon-Ginet, R. Cortes, and J. M. Dubois, J. Phys. (Paris) 43, 539 (1982).

<sup>20</sup>D. M. Pease, D. L. Brewster, Z. Tan, and J. I. Budnick, Phys. Lett. A 138, 230 (1989).

<sup>21</sup>C. Brizard and B. Rodricks, Rev. Sci. Instrum. 63, 802 (1992).